

BIOFABRICATION OF ZINC OXIDE NANOPARTICLES USING *PTEROCARPUS MARSUPIUM* AND ITS BIOMEDICAL APPLICATIONS

SHYMALA RAJAN ABHINAYA, RAMAKRISHNAN PADMINI*

Department of Biochemistry, School of Life Sciences, Vels Institute of Science, Technology and Advanced Studies, Chennai, Tamil Nadu, India.
Email: padmini.sls@velsuniv.ac.in

Received: 24 July 2018, Revised and Accepted: 25 September 2018

ABSTRACT

Objective: The objective of the study is to perform the synthesis of zinc oxide nanoparticles using the bark extract of *Pterocarpus marsupium* and to evaluate its biomedical applications.

Methods: Various concentrations of zinc acetate are used, and synthesis conditions were optimized to get a stable nanoparticle. The finest synthesis condition for zinc oxide nanoparticle production was at pH 7 with 20 ml extract, zinc acetate 10 mM, and 120 min of reaction time. The synthesized nanopowder was characterized using various analytical techniques, such as ultraviolet (UV)-visible spectroscopy, Fourier-transform infrared (FTIR) spectroscopy, X-ray diffraction (XRD), and scanning electron microscopy (SEM). The synthesized nanoparticles were tested for their antimicrobial, anti-inflammatory, inhibition of lipid peroxidation, and inhibition of amylase activity.

Results: The size range of nanoparticles obtained was in the range of 10–32 nm as reported by SEM. The UV-visible absorption spectrum of the synthesized nanoparticle showed a peak at 340 nm, which confirmed the presence of nanoparticles. FTIR spectroscopy analysis indicated the presence of zinc oxide stretching at 666.22 cm^{-1} . Further, the IR spectra indicated the presence of alcohols and acids, which can act as capping agents around the nanoparticles. XRD analysis confirmed the crystalline nature of nanoparticles.

The synthesized nanoparticle showed appreciable antimicrobial activity. Zinc oxide nanoparticles at 40 $\mu\text{g}/\text{well}$ were tested against phytopathogens, *Pseudomonas aeruginosa*, *Staphylococcus aureus*, *Aspergillus flavus*, and *Aspergillus niger* showed 16, 13, 15, and 16 mm zones of inhibition, respectively. The synthesized nanoparticle showed a considerable increase in inhibition of lipid peroxidation and amylase activity. The nanoparticle also exhibited appreciable anti-inflammatory activity measured by the inhibition of albumin denaturation.

Conclusion: The study instigates the simple and convenient method of synthesizing zinc oxide nanoparticles using *P. marsupium* and its few biomedical applications.

Keywords: Zinc oxide, Nanoparticles, *Pterocarpus marsupium*, Anti-inflammatory, Antimicrobial, Lipid peroxidation, Amylase inhibition.

© 2019 The Authors. Published by Innovare Academic Sciences Pvt Ltd. This is an open access article under the CC BY license (<http://creativecommons.org/licenses/by/4.0/>) DOI: <http://dx.doi.org/10.22159/ajpcr.2019.v12i1.28682>

INTRODUCTION

Nanotechnology is the science about the synthesis of nanosized materials of variable size, shapes, chemical composition, and its potential use for human benefits [1-3]. The various types of nanoparticles include the metal nanoparticles, metal oxide nanoparticles, and polymer nanoparticles. Of these, the metal oxide nanoparticles comprise the most versatile one, owing to the metal oxide's stability, improved unique physical and chemical properties, and diversity in functionalities. Recently, nanotechnology has immense application in the field of life sciences and medical sciences with special emphasis on biomedical devices and as therapeutics [4]. Nanoparticles synthesized using physical and chemical methods are pure, well-defined but pose certain limitations such as environmental threats and high cost, whereas the biological methods are cost-effective and eco-friendly. The green synthesis of nanoparticles is achieved using plants and their derivatives and microorganisms such as bacteria, fungi, algae, and yeast. *Pterocarpus marsupium* Roxb., a plant belonging to Fabaceae, is traditionally used in ayurvedic system for the treatment of diabetes [5]. *P. marsupium* is, also commonly known as Malabar kino or Indian kino tree or Vijayasar. The plant is a medium-to-large, deciduous tree that can grow up to 30 m (98 ft) tall. It is indigenous to India, Nepal, and Sri Lanka. The plant exhibits many pharmacological activities that include hepatoprotective, antioxidant, antimicrobial, antidiabetic, and anti-inflammatory activities [5,6]. The plant decreases the opacity index of

the diabetic retina, thus proving its anticataract activity [7]. It reduces inflammation by inhibiting cyclooxygenase 2 and thus decreasing the prostaglandin 2 production [8]. So far the plant has not been subjugated for nanoparticle fabrication and its application. This study emphasizes the production, characterization, and few of its biomedical applications of green-synthesized zinc oxide nanoparticles using *P. marsupium*.

METHODS

Collection of plant

The plant material *P. marsupium* was collected in and around Chennai and authenticated by Dr. P. Jayaraman, Plant Anatomy Research Centre, Chennai, India (voucher specimen no: PARC/2017/3307).

Preparation of zinc oxide nanoparticles using *P. marsupium*

Zinc oxide nanoparticles were synthesized using zinc acetate dihydrate $\text{Zn}(\text{CH}_3\text{COO})_2 \cdot 2\text{H}_2\text{O}$ as described previously by Gnanasangeetha and Thambavani 2013 [9] with slight modifications. Dried bark was ground to yield coarse powder, and 20 g of which was boiled in 100 ml of double-distilled water for 15 min. The aqueous extract was then cooled, filtered using Whatman No.1 filter paper, and stored at 4°C for further use.

Synthesis and optimization of zinc oxide nanoparticles

20% aqueous extract with increasing concentrations of zinc acetate (5, 6, 7, 8, 9, and 10 mM) was used to optimize the synthesis. The

mixture was heated constantly at 60°C with continuous stirring for 2 h. The solution was then dried in oven at 60°C. The concentration of 10 mM zinc acetate was fixed, since complete conversion to zinc oxide nanoparticles takes place during drying at this 10 mM concentration of zinc acetate. The synthesized zinc oxide nanopowder was stable even after 6 months.

Characterization studies

Optical properties of synthesized zinc oxide nanoparticle were characterized based on ultraviolet (UV) absorption spectra. The nanoparticles were diluted in deionized water (0.1 mg/ml), and the UV spectrum was recorded on Shimadzu UV-1800 spectrophotometer at the wavelength range of 200–500 nm. Infrared (IR) spectra of synthesized nanoparticles were recorded on a Bruker series Fourier-transform IR (FTIR) spectrometer using KBr pellets. The spectra were obtained within the frequency range of 4000–500cm⁻¹. X-ray diffraction (XRD) analysis was recorded on a Seifert 3000P X-ray diffractometer operating at 30 kV and 40 mA. The pattern was recorded by CuK α radiation with about 1.54060Å in steps of 0.02, with 2 θ scanning range from 10° to 80°. High-resolution scanning electron microscopy (SEM) was performed using JEOL 2100 field emission gun-based scanning electron high-resolution microscope to analyze the nanoparticle shape and size.

In vitro antibacterial and antifungal activity

Bacteria, namely *Pseudomonas aeruginosa* and *Staphylococcus aureus*, were maintained at 4°C on nutrient agar slants. Overnight bacterial cultures grown in nutrient broth were adjusted to an inoculum size of 10⁸ cells/ml for inoculation of the agar plates. An aliquot (0.2 ml) of inoculum was added to the nutrient agar medium (HiMedia). The growth inhibition of bacteria by the nanoparticle was determined by the agar well diffusion assay as described by Kudi *et al.* [10]. Bacteria were maintained at 37°C on nutrient agar plates before use. Nutrient agar was prepared and 25 ml each was poured into a sterile Petri dish. This was allowed to solidify and dry. Using a sterile cork borer of 8-mm diameter, three equidistant holes per plate were made in the agar and were inoculated with 0.2 ml overnight suspension of the bacteria. The wells (holes) were filled with the synthesized nanoparticle solution at varying concentrations of 10 mg/ml, 5 mg/ml, and 2.5 mg/ml, respectively. The plates were incubated at 37°C for 24 h. The experiments were repeated thrice. The antibacterial activities were observed and measured using a transparent meter rule and recorded if the zone of inhibition was ≥ 10 mm [10,11]. The nanoparticles were also tested in a similar manner against fungal pathogens, namely *Aspergillus flavus* and *Aspergillus niger*.

In vitro lipid peroxidation

A modified thiobarbituric acid (TBA) reactive species assay was used to measure the lipid peroxide formed using liver homogenates as lipid-rich media, as described by Ruberto *et al.* [12]. Briefly, 0.5 ml of liver homogenate (10% v/v) was added to 0.1 ml of the synthesized zinc oxide nanoparticle (10 μ g/ml). The volume was then made up to 1.0 ml with distilled water. Thereafter, 0.05 ml of FeSO₄ was added and the mixture was incubated at 37°C for 30 min. Then, 1.5 ml of acetic acid was added, followed by 1.5 ml of TBA in sodium dodecyl sulfate. The resulting mixture was mixed thoroughly and heated at 95°C for 1 h. After cooling, 5 ml of butanol was added and the mixture was centrifuged at 3000 rpm for 10 min. The optical density of the organic upper layer was measured at 532 nm. The percentage inhibition was calculated with the formula:

$$\% \text{ inhibition of lipid peroxidation} = \left[\frac{100 - A_{\text{sample}}}{A_{\text{control}}} \right] \times 100$$

Assay of alpha-amylase inhibition

Alpha-amylase inhibitory activity of synthesized zinc oxide nanoparticle was analyzed by the method of Bernfeld, 1995 [13]. Briefly, 100 μ l of the synthesized zinc oxide nanoparticle was allowed to react with 200 μ l of

α -amylase enzyme and 100 μ l of 2 mM phosphate buffer (pH 6.9). After 20-min incubation, 100 ml of 1% starch solution was added. The same was performed for the control where 200 μ l of the enzyme was replaced by buffer. After incubation for 5 min, 500 μ l of the dinitrosalicylic acid reagent was added to both control and test. They were kept in a boiling water bath for 5 min. The optical density was recorded at 540 nm using a spectrophotometer. The percentage inhibition of α -amylase enzyme was calculated using the following formula:

$$\text{Inhibition (\%)} = 100 \times \left[\frac{\text{Control} - \text{Test}}{\text{Control}} \right]$$

Inhibition of albumin denaturation

The synthesized compounds are screened for anti-inflammatory activity using inhibition of albumin denaturation technique, which was studied according to Mizushima and Kobayashi (1968) with slight modification [14]. The standard drug and synthesized nanoparticles dissolved in a minimum amount of dimethylformamide (DMF) and diluted with phosphate buffer (0.2 M, pH 7.4). The final concentration of DMF in all solutions was <2.5%. Test solution (1 ml) containing different concentrations of nanoparticles was mixed with 1 ml of 1 mM albumin solution in phosphate buffer and incubated at 27°C \pm 1°C in BOD incubator for 15 min. Denaturation was induced by keeping the reaction mixture at 60°C \pm 10°C in a water bath for 10 min. After cooling, the turbidity was measured at 660 nm (UV-visible spectrophotometer, Shimadzu). Percentage of the inhibition of denaturation was calculated from the control where no drug was added. Each experiment was done in triplicate and the average was taken. The diclofenac sodium was used as standard drug.

Statistical evaluation

All results are expressed as mean \pm SEM (n=6). IC₅₀ values were calculated by applying suitable regression analysis of the mean inhibitory values.

RESULTS

IR spectra

The IR spectra of *P. marsupium* zinc oxide nanoparticles are shown in Fig. 1. The IR spectra are recorded in the mid-IR region within the range (400–4500cm⁻¹). The FT-IR spectra resulted in various peaks at 3298.92, 2917.86, 2113.41, 1988.50, 1932.31, 1618.54, 1423.48, 1251.71, 1020.33, 767.23, and 666.22cm⁻¹.

UV visible spectra

Fig. 2 represents the UV-visible absorption spectrum of *P. marsupium* ZnO nanoparticles. A strong absorption band at about 340nm clearly demonstrates the presence of ZnO nanoparticles in the reaction mixture [15].

XRD

The XRD spectrogram of *P. marsupium* zinc oxide nanoparticles is shown in Fig. 3. The distinctive ZnO peaks with corresponding miller indices

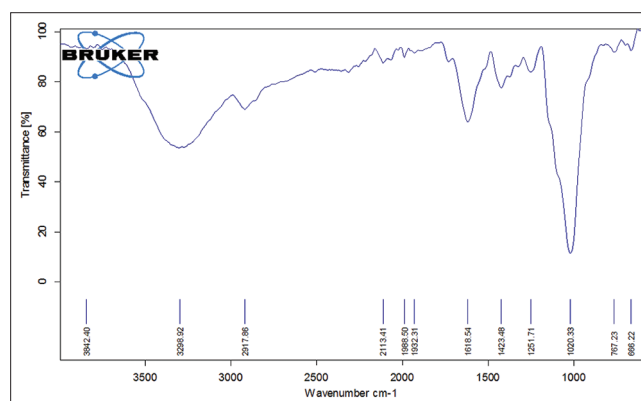


Fig. 1: Infrared spectrum of zinc oxide nanoparticles synthesized using *Pterocarpus marsupium*

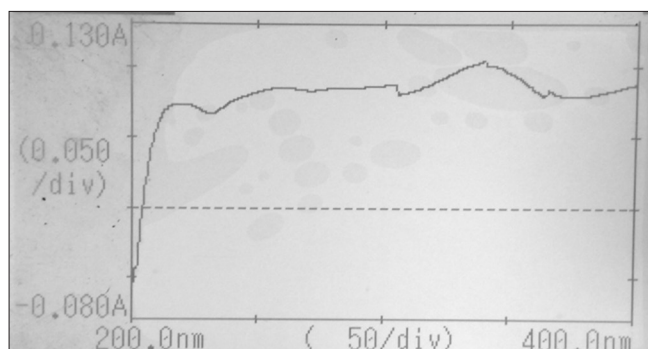


Fig. 2: Ultraviolet spectrum of zinc oxide nanoparticles synthesized using *Pterocarpus marsupium*

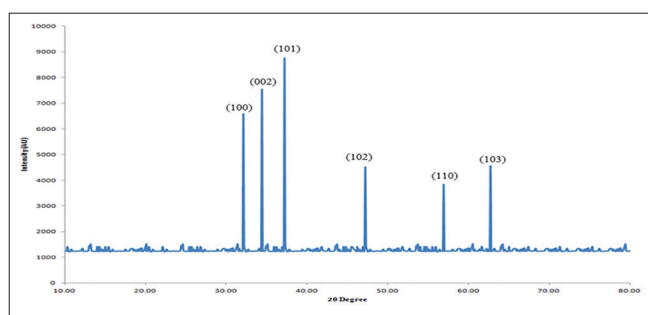


Fig. 3: X-ray diffraction spectrum of zinc oxide nanoparticles synthesized using *Pterocarpus marsupium*

are as follows at 32.90 (100), 34.5 (002), 36.33 (101), 47.50 (102), 57.25 (110), and 63.62 (103), respectively.

SEM

Fig. 4 represents the SEM pictures of *P. marsupium* ZnO nanoparticles at $\times 60,000$ magnifications. The SEM images confirm the formation of ZnO nanoparticles. The images also clearly substantiate the approximate spherical shape to the nanoparticles.

Antimicrobial activity

Tables 1 and 2 represent the antibacterial and antifungal activity of *P. marsupium* zinc oxide nanoparticles. The synthesized zinc oxide nanoparticles showed an appreciable antibacterial activity on *P. aeruginosa* and *S. Aureus* and antifungal activity on *A. flavus* and *A. niger* strains (Table 3 and Fig. 5).

Effect on lipid peroxidation

The synthesized ZnO nanoparticle demonstrated a considerable amount of lipid peroxidation inhibitory effect by 59.03%, while butylated hydroxy anisole significantly inhibited lipid peroxidation by 64.43% at the concentration of 100 $\mu\text{g/ml}$. The results were concentration dependent as depicted in Table 3. The IC_{50} was found to be 177.53 for synthesized zinc oxide nanoparticles.

Effect on amylase inhibition

Table 4 represents the amylase inhibitory activity by *P. marsupium* zinc oxide nanoparticles. The percentage inhibition of alpha-amylase by the ZnO nanoparticle synthesized using *P. marsupium* was studied in a concentration range of 20–100 $\mu\text{g/ml}$, and the IC_{50} was found to be 59.38.

Effect on protein denaturation

The *in vitro* anti-inflammatory activity of *P. marsupium* zinc oxide nanoparticle on inhibiting denaturation of proteins is clearly depicted in Table 5. The minimum inhibition by the synthesized nanoparticles is $20.20 \pm 1.18\%$ observed at the concentration of 20 $\mu\text{g/ml}$. The IC_{50} was found to be 98.45.

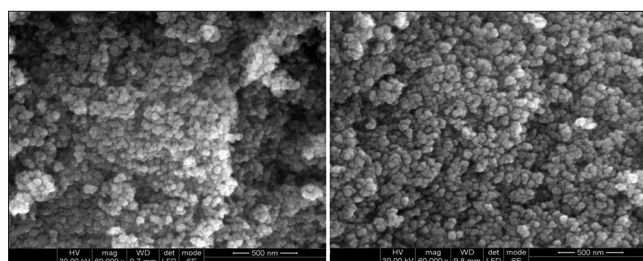


Fig. 4: Scanning electron micrograph of zinc oxide nanoparticles synthesized using *Pterocarpus marsupium*

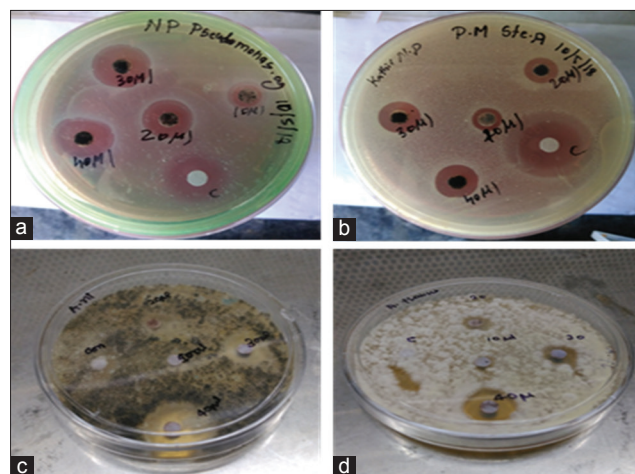


Fig. 5: Antibacterial and antifungal activity of zinc oxide nanoparticles synthesized using *Pterocarpus marsupium*. Bacterial strains - (a) *Pseudomonas aeruginosa* and (b) *Staphylococcus aureus*; Fungal strains - (c) *Aspergillus niger* and (d) *Aspergillus flavus*

DISCUSSION

IR spectrum

FT-IR spectroscopy helps to establish the identity of various phytochemical constituents involved in the reduction and stabilization of the nanoparticles. In this study, the peak around 3298.92cm^{-1} corresponds to alcohols (O-H). The peaks at 2917.86 and 2113.41cm^{-1} denote SP 3 carbon-hydrogen/alkyl (C-H). The peaks at 2113.41cm^{-1} correspond to alkyne (C \equiv C) group. The peak at 1618.54cm^{-1} denotes alkene (C=C).

The absorption peaks in the range of $400\text{--}700\text{cm}^{-1}$ are attributed to the ZnO stretching modes. Depending on the synthesis and other experimental conditions, weak bands for zinc oxide are positioned at 520cm^{-1} , 566cm^{-1} , and 665cm^{-1} [16,17]. A peak at 666.22cm^{-1} obtained in this study is suggestive of zinc oxide stretching.

UV-visible spectrum

UV spectrum is widely being used to examine the optical properties of nanosized particles. Conducting electrons begin oscillating at a certain wavelength range due to surface plasmon resonance effect. In this study, an absorption peak is observed at 340 nm. This result is in concordance with report of Elizabeth Varghese and Mary George, 2015, where the blue shift in the absorption spectrum at 340 nm is suggestive of the formation of zinc oxide nanoparticles [15].

XRD

The 2θ values obtained in this study are exactly located at 34.52° , 36.33° , 47.5° , and 63.6° . The spectrum is comparable to the hexagonal Wurtzite phase of zinc oxide [18,19] (JPCDS card number: 36-1451).

Table 1: Antifungal activity of *Pterocarpus marsupium* zinc oxide nanoparticles

Organism	Positive control	40 µg	10 µg	Negative control (zinc acetate alone)
<i>Aspergillus flavus</i>	21	16	7	10
<i>Aspergillus niger</i>	19	13	6	10

Table 2: Antibacterial activity of *Pterocarpus marsupium* zinc oxide nanoparticles

Organism	Positive control	40 µg	10 µg	Negative control (zinc acetate alone)
<i>Escherichia coli</i>	20	15	7	10
<i>Pseudomonas aeruginosa</i>	21	16	7	10

Table 3: *In vitro* lipid peroxidation by *Pterocarpus marsupium* zinc oxide nanoparticles

Treatment	Concentration	% inhibition	IC ₅₀
<i>Pterocarpus marsupium</i> zinc oxide nanoparticles	20	21.0±1.15	177.53
	40	36.6±0.89	
	60	45.0±1.53	
	80	51.33±1.66	
	100	59.03±0.92	
BHA	20	25.7±1.27	78.49
	40	32.2±1.54	
	60	45.5±1.31	
	80	54.4±1.77	
	100	64.4±1.85	

Values are expressed in terms of mean±Standard Error of Mean (n=6). BHA: Butylated hydroxy anisole.

Table 4: Amylase inhibitory activity by *Pterocarpus marsupium* zinc oxide nanoparticles

Treatment	Concentration	% inhibition	IC ₅₀
<i>Pterocarpus marsupium</i> zinc oxide nanoparticles	40	33.36±1.31	59.38
	60	44.93±1.83	
	80	56.03±1.62	
	100	59.23±1.61	
Acarbose	20	21.0±1.05	218.49
	40	30.76±1.76	
	60	42.73±1.61	
	80	52.36±1.88	
	100	64.26±2.12	

Values are expressed in terms of mean±Standard Error of Mean (n=6).

Table 5: Inhibition of protein denaturation by *Pterocarpus marsupium* zinc oxide nanoparticles

Treatment	Concentration	% inhibition	IC ₅₀
<i>Pterocarpus marsupium</i> zinc oxide nanoparticles	20	20.20±1.18	98.45
	40	36.23±1.15	
	60	48.53±1.48	
	80	56.33±1.24	
	100	64.63±1.50	
Diclofenac sodium	20	13.83±1.07	167.23
	40	36.56±1.41	
	60	59.43±1.56	
	80	73.3±1.76	
	100	90.83±2.02	

Values are expressed in terms of mean±Standard Error of Mean (n=6).

SEM

The synthesized zinc oxide nanoparticles are spherical in shape, and most of the particles exhibit some faceting. This spherical shape is similar to the reports of Raj and Jayalashmi, 2015 [20].

Antimicrobial activity

Antimicrobial activity of ZnO nanoparticles against various pathogens such as *Bacillus subtilis*, *Salmonella*, *Listeria monocytogenes*, *S. aureus*, and *Escherichia coli* using disc diffusion method has been reported [21,22]. The antimicrobial activity of *P. marsupium* is also well documented [23]. In this study, the zones of inhibition recorded (in mm) for *P. aeruginosa*, *S. aureus*, *A. flavus*, and *A. niger* are 16, 13, 15, and 16 at 40 µg/ml well, respectively (Fig. 5), suggesting that *P. marsupium* synthesized zinc oxide nanoparticles are also effective in culminating the microbial growth. Some of the proposed mechanisms of antibacterial activity by the zinc oxide nanoparticles include the disruption of the cell membrane, oxidative stress induction and generation of reactive oxygen species, Zn⁺⁺ release, internalization of ZnO NPs into bacteria, and electrostatic interactions as reported by Sirelkhatim *et al.*, 2015 [24].

Inhibition of lipid peroxidation

Lipid peroxidation is the process by which the free radicals obtain electrons from the lipids in cell membranes and cause the oxidative degradation of lipids culminating in cell damage. In this study, the peroxidation of liver phospholipid extract was induced by ferric chloride. The hydroxyl radicals formed during the reaction interact with biological membranes, leading to the formation of malondialdehyde and other aldehydes that form a pink chromogen with TBA, showing strong absorbance at 532 nm. In this study, *P. marsupium* synthesized zinc oxide nanoparticles showed an appreciable effect on the inhibition of lipid peroxidation. Furthermore, *P. marsupium* has been reported to have antioxidant property [5,23]. The phenolic compounds in the plant extract may suppress lipid peroxidation through different chemical mechanisms, including free radical quenching, electron transfer, radical addition, or radical recombination [25], thus suggesting its role in inhibition of lipid peroxidation.

Amylase inhibition

Alpha-amylase is an enzyme involved in starch breakdown, and the inhibition of amylase activity is a further therapeutic target in controlling type II diabetes. Plant-based α-amylase inhibitors control the rate of digestion and absorption of carbohydrates [26]. Zinc oxide nanoparticles as possible alpha-amylase inhibitors have well been documented, wherein the optimum dose of 20 µg/ml was sufficient to exhibit 49% glucose inhibition at neutral pH and 35°C temperature [27].

Inhibition of protein denaturation

Denaturation of protein means loss of biological properties of protein molecules, its structure as well its function. Protein denaturation is a consequence of inflammation. Production of autoantigens in certain arthritic diseases may be due to the denaturation of proteins *in vivo* [28,29]. Drugs or phytochemicals which are helpful in preventing protein denaturation are promising anti-inflammatory therapeutics [30]. The anti-inflammatory effects are mediated by phenolics and flavonoids present in the plant extracts [31]. In this study, we observed a dose-dependent inhibition of protein denaturation by the zinc oxide nanoparticles. This is suggestive of its anti-inflammatory effect. The ability to inhibit protein

denaturation is indirectly serving the ailment to mitigate, and this could serve as a target for anti-inflammatory drug development.

CONCLUSION

The method used for the synthesis of zinc oxide nanoparticle using *P. marsupium* is both energy and cost-effective with a high particle yield at lower concentration of plant extract. The synthesized nanoparticles are highly stable. The FTIR spectrum showed the ZnO stretching at 666 cm^{-1} and the optical property measured by UV spectroscopy with absorption peak maximum at 340 nm. XRD confirmed the crystalline nature of nanoparticles. The morphology of synthesized nanoparticles assessed by SEM clearly enunciates its spherical nature with size ranging from 10 to 32 nm. The synthesized nanoparticle was further studied for few biomedical applications. The nanoparticles showed appreciable antimicrobial activity. The *in vitro* inhibition of amylase activity, albumin denaturation, and lipid peroxidation by the synthesized ZnO nanoparticle makes it a potential therapeutic against inflammation disorders.

CONFLICTS OF INTEREST

They have no conflicts of interest.

AUTHORS' CONTRIBUTION

(1) Shymala Rajan Abhinaya performed the experiments presented in this study. (2) Ramakrishnan Padmini devised the concept and plan of the study, interpretation of the data obtained, and preparation of the manuscript.

REFERENCES

- Colvin VL, Schlamp MC, Alivisatos A. Light emitting diodes made from cadmium selenide nanocrystals and a semiconducting polymer. *Nature* 1994;370:354-57.
- Wang Y, Herron N. Nanometer-sized semiconductor clusters: Materials synthesis, quantum size effects, and photophysical properties. *J Phys Chem* 1991;95:525-32.
- Schmid G. Large clusters and colloids. *Metals in the embryonic state*. *Chem Rev* 1992;92:1709-27.
- Hoffman AJ, Mills G, Yee H, Hoffmann M. Q-sized cadmium sulfide: Synthesis, characterization, and efficiency of photoinitiation of polymerization of several vinylic monomers. *J Phys Chem* 1992;96:5546-52.
- Abhishek N, Hegde K. Pharmacological profile of *Pterocarpus marsupium* with a note on its therapeutic activity. *Int J Pharm Clin Res* 2017;3 Suppl 1:32-7.
- Manikani KL, Krishna V, Manjunatha BK, Vidya SM, Singh SD, Manohara YN, et al. Evaluation of hepatoprotective activity of stem bark of *Pterocarpus marsupium* Roxb. *Indian J Pharmacol* 2005;37 Suppl 3:165-8.
- Vats V, Yadav SP, Biswas NR, Grover JK. Anti-cataract activity of *Pterocarpus marsupium* bark and *Trigonella foenum-graecum* seeds extract in alloxan diabetic rats. *J Ethnopharmacol* 2004;93 Suppl 2-3:289-94.
- Hougee S, Faber J, Sanders A, Dejong RB, Vandenberg WB, Garssen J, et al. Selective COX-2 inhibition by a *Pterocarpus marsupium* extract characterized by pterostilbene, and its activity in healthy human volunteers. *Planta Med* 2005;71 Suppl 5:387-92.
- Gnanasangeetha D, Thambavani SD. Biogenic production of zinc oxide nanoparticles using *Acalypha indica*. *J Chem Biol Phys Sci* 2014;4 Suppl 1:238-46.
- Kudi AC, Umoh JU, Eduvic LO, Getu J. Screening of some Nigerian medicinal plants for antibacterial activity. *J Ethnopharmacol* 1999;67:225-8.
- Vlietink AJ, Van Hoof L, Totte J, Laure H, Vanden Berhe D, Rwangabo PC, et al. Screening of hundred rwandese medical plants for antimicrobial and antiviral properties. *J Ethnopharmacol* 1995;46:31-47.
- Ruberto G, Baratta MT, Deans SG, Dorman HJ. Antioxidant and antimicrobial activity of *Foeniculum vulgare* and *Crithmum maritimum* essential oils. *Planta Med* 2000;66:687-93.
- Bernfeld P. Amylases, α and β . *Methods Enzymol* 1955;1:149-58.
- Mizushima Y, Kobayashi M. Interaction of anti-inflammatory drugs with serum proteins, especially with some biologically active proteins. *J Pharm Pharmacol* 1968;20:169-173.
- Varghese E, George M. Green synthesis of zinc oxide nanoparticles. *Int J Adv Res Sci Eng* 2015;4 Suppl 1:307-14.
- Djaja N, Montja D, Saleh R. The effect of Co incorporation into ZnO nanoparticles. *Adv Mater Phys Chem* 2013;3 Suppl 1:33-41.
- Hernández A, Maya L, Sánchez-Mora E, Sánchez EM. Sol-gel synthesis, characterization and photocatalytic activity of mixed oxide ZnO-Fe₂O₃. *J Solgel Sci Technol* 2007;42 Suppl 1:71-8.
- Zhou J, Zhao F, Wang Y, Zhang Y, Yang L. Size-controlled synthesis of ZnO nanoparticles and their photoluminescence properties. *J Lumin* 2007;122-3 Suppl 1-2:195-7.
- Khoshhesab ZM, Sarfaraz M, Asadabad MA. Preparation of zno nanostructures by chemical precipitation method. *Synth React Inorg Met Org Nano Met Chem* 2011;41 Suppl 7:814-9.
- Raj LF, Jayalakshmy E. A biogenic approach for the synthesis and characterization of zinc oxide nanoparticles produced by *Tinospora cordifolia*. *Int J Pharm Pharm Sci* 2015;7 Suppl 8:384-6.
- Fowsiya J, Madhumitha G, Al-Dhabi NA, Arasu MV. Photocatalytic degradation of Congo red using *Carissa edulis* extract capped zinc oxide nanoparticles. *J Photochem Photobiol B* 2016;162:395-401.
- Dobrucka R, Długaszewska J. Biosynthesis and antibacterial activity of ZnO nanoparticles using *Trifolium pratense* flower extract. *Saudi J Biol Sci* 2016;23:517-23.
- Deepa R, Manjunatha H, Krishna V, Swamy BE. Evaluation of antimicrobial activity and antioxidant activity by electrochemical method of ethanolic extract of *Pterocarpus marsupium* Roxb bark. *J Biotechnol Biomater* 2014;4:166-9.
- Sirelkhatim A, Mahmud S, Seeni A, Kaus NH, Ann LC, Bakhori SK, et al. Review on zinc oxide nanoparticles: Antibacterial activity and toxicity mechanism. *Nano Micro Lett* 2015;7 Suppl 3:219-42.
- Hodges DM, DeLong JM, Forney CF, Prange RK. Improving the thiobarbituric acid-reactive-substances assay for estimating lipid peroxidation in plant tissues containing anthocyanin and other interfering compounds. *Planta* 1999;207:604-11.
- Musa MY, Griffith AM, Michels AJ, Schneider E, Frei B. Inhibition of α -amylase and α -glucosidase activity by tea and grape seed extracts and their constituent catechins. *J Agric Food Chem* 2012;60:8924-9.
- Dhobale S, Thite T, Laware SL, Rode CV, Koppikar SJ, Ruchika-Kaul G, et al. Zinc oxide nanoparticles as novel alpha-amylase inhibitors. *J App Phys* 2008;104:94907.
- Leelaprakash G, Dass SM. *In vitro* antiinflammatory activity of methanol extract of *Enicostemma axillare*. *Int J Drug Dev Res* 2010;3:189-96.
- Ingle PV, Patel DM. C-reactive protein in various disease condition-an overview. *Asian J Pharm Clin Res* 2011;4 Suppl 1:9-13.
- Phongpradist R, Chaiyana W, Anuchapreeda S. Curcumin-loaded multi-valent ligands conjugated-nanoparticles for anti-inflammatory activity. *Int J Pharm Pharm Sci* 2015;7 Suppl 4:203-8.
- Sangeetha G, Vidhya R. *In vitro* anti-inflammatory activity of different parts of *Pedaliium murex* (L.) *Int J Herb Med* 2016;4 Suppl 3:31-6.